



DYNAMIC POSITIONING CONFERENCE
October 17 – 18, 2000

DESIGN

Model Tests for the DPS of the OD21 Drillship

Isao Yoshino
Mitsui Engineering and Shipbuilding Co., Ltd. (Chiba, Japan)

Kazuyuki Igarashi
Akishima Laboratories (Mitsui Zosen) Inc. (Tokyo, Japan)

Shinichi Takagawa & Yasutaka Amitani
Japan Marine Science and Technology Center (Yokosuka, Japan)

1 Introduction

It is necessary to keep a vessel's position within the required distance from the decided position such as the position right above a drilling hole in drilling operations. As the OD21 (Ocean Drilling in the 21st Century) project¹⁾ aims a deepwater scientific ocean drilling up to 4000m water depth in case of a riser drilling and 7000m water depth in case of a riserless one, DPS is the only solution for the position keeping of the OD21 drillship. In general, high capability and reliability are required for the DPS in riser drilling operations. Detailed investigations have been, therefore, carried out for the capability and reliability of the DPS. In this connection, several model tests have been conducted at basins of the Akishima Laboratories (Mitsui Zosen) Inc. in Tokyo, Japan.

DP control logic of the actual (full scale) DPS is usually, in a sense, "a black box" for an owner, shipyard and laboratory, because the logic is involved in a confidential know-how by a DPS manufacturer. Mitsui Engineering & Shipbuilding Co., Ltd. is, however, not only a shipyard but also a DPS manufacturer who fully utilizes the own possessed Akishima Laboratories. The DP control logic is, therefore, no more "a black box" for the authors and the model tests have been able to be successfully performed with our intellect and experience. As a matter of fact, the DPS of the OD21 drillship has been developed based on such an intellect and experience with use of the model test results.

This paper describes mainly the model tests for the DPS and briefly the overview of the OD 21 project and features of the vessel.

2 Overview of the OD21 project

The project of the OD 21 is a new Japanese project of a deepwater scientific ocean drilling for the 21st century. This new drilling project will take upon the major part of the Integrated Ocean Drilling Program (IODP) succeeding the ongoing Ocean Drilling Program (ODP, 1985-2003). The project is not a commercial one but purely a scientific one to contribute to the international scientific community through developments of the physical geography of the Earth. From a software aspect, the project aims the construction of an international research base for those who will be engaged in physical geography researches, and also includes the training of young researchers. On the other hand, the main target of the project from a hardware aspect is to construct a new drillship equipped with the facilities of a riser drilling and onboard laboratory so as to achieve the objectives of the project described below.

Application of the riser system enables the vessel, with safety and high core-recovery rates, to drill through the potentially hydrocarbon-containing layer and the high stress layer, which the present project ODP cannot drill through because of its riserless drilling. The OD 21, therefore, makes it possible to widen the areas and depths available to be researched. In addition, the deepwater drilling may enable us to eventually reach the mantle and to monitor the deep interior of the Earth throughout borehole windows. Objectives of the OD 21 are as follows;

- Precise reconstruction of the Earth's past environmental changes
- Establishment of a whole-Earth tectonics theory
- Understanding plate-subduction dynamics
- Developing natural disaster prediction capabilities

Basic design of the OD 21 drillship was started in 1999, under a consultation of the Japan Marine Science and Technology Center as an owner, by the Mitsui Engineering and Shipbuilding Co., Ltd. and the Mitsubishi Heavy Industries Ltd. Mitsui is in charge of hull, accommodation, onboard laboratory and DPS, while Mitsubishi is in charge of drilling units and subsea systems. The construction of the vessel will be started in 2001 after the detailed design, which is currently performed by the same parties. Her completion will be planned in early 2004.

3 Features of the OD21 drillship

3.1 Main features

The OD 21 drillship is designed to apply the state of the art drilling technologies in order to comply with the scientific deepwater drilling required. The vessel is equipped with the onboard laboratories capable of researching the physical geography. In addition, special considerations are being taken for countermeasures for environmental pollution and disruption so that the disposal treatment system for the waste mud, drilling drain and cuttings is under planning so as to be installed in near future. Such waste material will be transported by supply boats etc., to inland where it is finally treated and abandoned. The other main features of the vessel are as follows;

- Six (6)-month riser drilling operation with consumables supplied by two(2) weeks
- 70 day riserless drilling operation without any supply
- Working worldwide with the high DP performance
- Long-distance voyages with the good maneuverability
- Riser system to endure high strength up to 2500 m waterdepth (to be made deeper up to 4000 m in near future)
- Acoustic positioning systems up to 7000 m waterdepth
- Course keeping and riser hang-off performance within 30 degrees off the bow up to the maximum wave height of 32 m and the one (1) minute average wind speed of 100 knots in survival condition corresponding to the 100-year return-period storm in the North Sea
- Wire line coring system suitable for the scientific drilling in order to obtain long cores
- Dual activity and dual hoist to improve drilling efficiency (to be applied in near future)
- Four (4) drill pipe and triple (3) casing pipe setback on the drill floor for reducing handling time
- Permanent drill pipe setback even in survival condition
- Direct tensioner for risers suitable for large capacity and free from fatigue of ropes
- Four (4) multi-knuckled jib cranes and one (1) conventional jib crane for helicopter deck

- Riser angle positioning system being newly developed for the project in order to decide the optimum vessel position to minimize the upper and lower riser angle without any information from the position sensors^{2),3)}
- Integrated management system for operational and laboratory information

3.2 Principal particulars and arrangement

The vessel is designed and sized to take the above-mentioned main features into account. **Table 1** highlights the principal particulars of the vessel.

Table 1 Principal particulars

Length overall	:	210.0 m
Length between perpendiculars	:	192.0 m
Breadth (moulded)	:	38.0 m
Depth (moulded)	:	16.2 m
Design draft (moulded)	:	9.2 m
Variable load	:	approx. 25,500 tons
Moonpool dimensions	:	L x B = approx. 21.9 m x 12.0 m
Complement	:	150 persons
Generators	:	5,000 kW x 6 sets + 2,500 kW x 2 sets
Thrusters (electric -driven)	:	4,200 kW x 6 sets (azimuth type) 2,550 kW x 1 set (tunnel type)

The general arrangement and 3-D model are shown in **Figure 1**. The vessel is a monohull type with double hull and double bottom having the rectangular shaped moonpool located near amidships. The superstructure consists of the derrick, substructure, drillfloor, accommodation, onboard laboratory, helicopter deck, fore castle deck, poop deck and the modules in which the drilling and subsea units are installed. One (1) riser rack and three (3) drill/casing pipe racks are fitted on the modules and the passageways run beside both sides of the modules from the accommodation fore to the poop aft. The derrick and drillfloor are designed to be suitable for dual handling future operation, and to endure the survival condition described above. The onboard laboratories arranged in the aft of the accommodation area consist of three decks containing the core processing unit, geochemistry laboratory and so on.

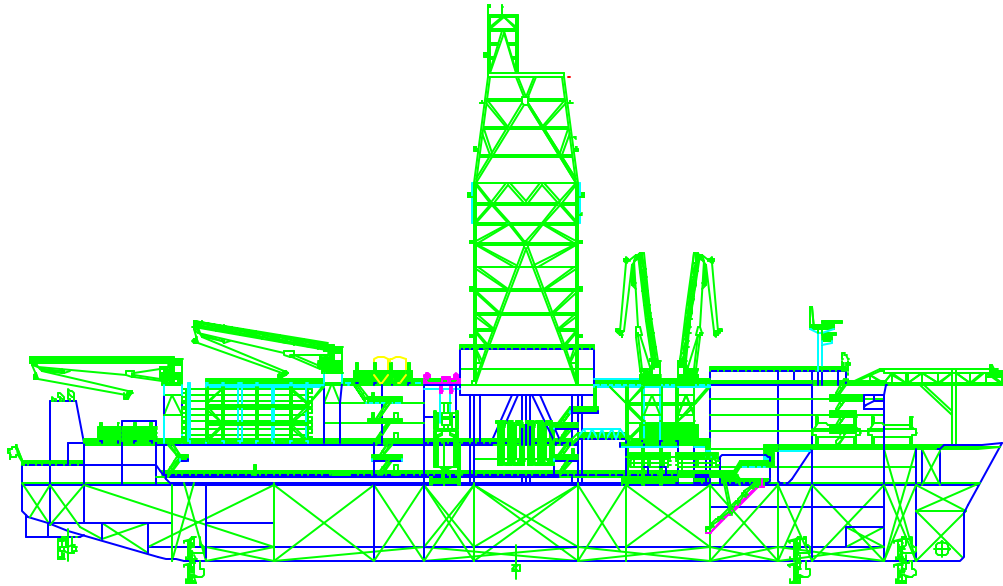


Figure 1 General arrangement and 3-D model of the OD21 drillship

3.3 Power generation and DPS

The power generation is located in two engine rooms aft under the upper deck. All generators and alternators described in [Table 1](#) are arranged in the engine rooms segregated on both sides by the A-60 and watertight bulkhead. In the engine rooms are also arranged three (3) azimuth thrusters, two (2) of which are not retractable ones located above the baseline. On the other hand, although another aft and three (3) fore azimuth thrusters are protruding below the baseline, they are designed to be retractable. The vessel is, therefore, capable of maneuvering in shallow waters with the two (2) non-retractable aft thrusters as well as the fore tunnel thruster.

Although the DPS is assigned the NK Class Notation DPS-B, further redundancy than required by the class is taken into account such as the segregation of the engine rooms described above, triple CPU of the computers and so on. The design conditions for the DPS are shown in [Table 2](#). The thrusters are sized and arranged so as to meet the DP performance in the environmental conditions of the Table 2. Among the conditions, the heading and location keeping capability against the survival condition is estimated to be the most stringent for sizing thrusters according to the dynamic simulation studies based upon the model tests described later. In other words, the thruster power is designed to reserve enough margins to keep the vessel's excursion within the limit of the drilling and standby condition in the [Table 2](#).

Table 2 Design conditions for the DPS

Condition name	Drilling condition	Standby condition 1	Standby condition 2	Survival condition
One(1) minute average wind speed (V_{w_1min})	23m/s	30m/s	23m/s	51.5m/s
Significant wave height ($H_{1/3}$)	4.5m	5.5m	5.5m	16m
Mean wave period (T_{01})	8.2sec	9.0sec	9.0sec	15.4sec
Current speed	1.5kts	1.5kts	2.5kts	2.5kts
Direction of wind/wave/current (off the bow)	30deg	30deg	30deg	within 30deg
Subject of control	Heading & positioning	Heading & positioning	Heading & positioning	Heading & location keeping
Thruster out of order	Any one	None	None	None
Allowable excursion in case of the DGPS for the position sensor	1.0% W.D. or 15m, whichever is more	2.0% W.D. or 30m, whichever is more	2.0% W.D. or 30m, whichever is more	None

(Note) W.D. : water depth

If the vessel has enough thrust to counter the static environmental forces, the vessel can stay on location statically. Excursion of the vessel cannot be, however, guaranteed due to dynamic effect such as gust wind, when the thruster power is limited within such static thrust. 20% thrust margin is, therefore, taken into account in the DP static simulations in addition to the thrust to counter the static environmental forces. It has been verified by means of the DP dynamic simulations that the 20% thrust margin in the static simulations is sufficient enough to keep the allowable excursion under the environmental conditions

shown in the Table 2 above. Concerning the DP capability, Figure 2 shows the allowable significant wave height obtained from the static simulations. Sea state of the North Pacific Ocean⁴⁾ is adopted as the relation between the wave height and wind speed, which corresponds to the relation of “Standby condition 2” above.

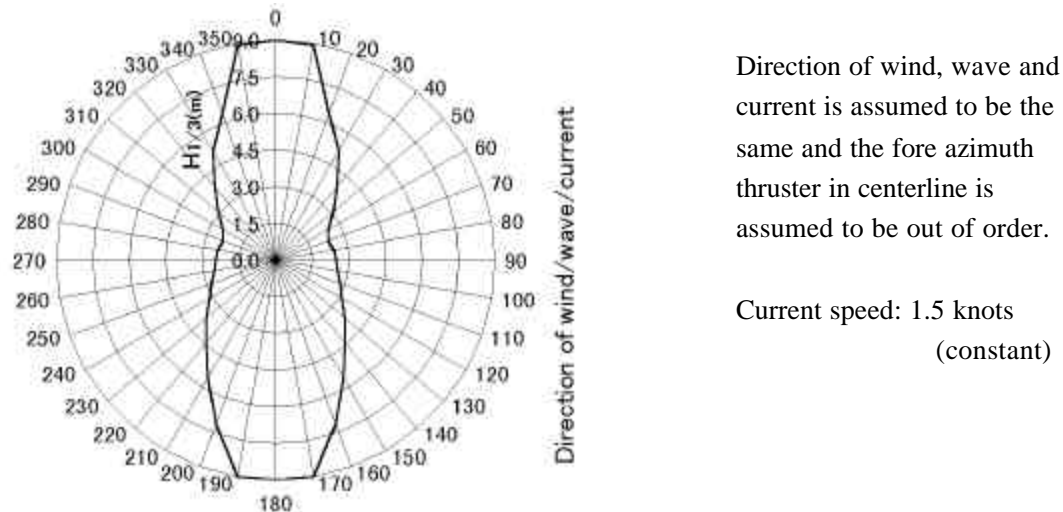


Figure 2 Allowable max. significant wave height in the North Pacific Ocean

4 Model tests for simulations

4.1 Overview

In the basic design stage of the DPS, various investigations concerning the DP capability and reliability have been carried out based on the above-mentioned static and dynamic simulations. For the sake of simulations, environmental force data such as wind, wave and current are required as well as maneuverability data at low vessel speed during the DP operations. Moreover for further accurate simulations, the simulations are to take account of interaction effects such as a thruster-hull interaction, thruster-current interaction with attack angle and so on. In order to obtain such hydrodynamic data, the wind tunnel tests, wave drift force tests, current tests, yaw-rotating tests and thruster interaction tests have been conducted. In addition, the other tests than the above have been also widely executed, e.g. the resistance tests, maneuverability tests, and cavitation tests with underwater noise measurements, explanation of which is omitted in this paper.

4.2 Mathematical model for dynamic simulation

The mathematical model for the DP simulations is represented on the basis of coupled equations of surge, sway and yaw. As a vessel moves in the horizontal plane with forward speed u , lateral speed v and rotational yaw rate r , the equations of motion are given by;

$$\text{Surge} : (m+m_x) \dot{u} - (m+m_y) vr = X_W + X_D + X_H + X_T$$

$$\begin{aligned} \text{Sway} : (m+m_y) \dot{y} + (m+m_x) ur &= Y_W + Y_D + Y_H + Y_T \\ \text{Yaw} : (I_{zz}+J_{zz}) \dot{r} &= N_W + N_D + N_H + N_T \end{aligned}$$

In the equations above, the terms with subscript W, D, H and T represent the wind forces, wave drift forces, hull forces and thruster forces respectively. Figure 3 gives a coordinate system used in this paper.

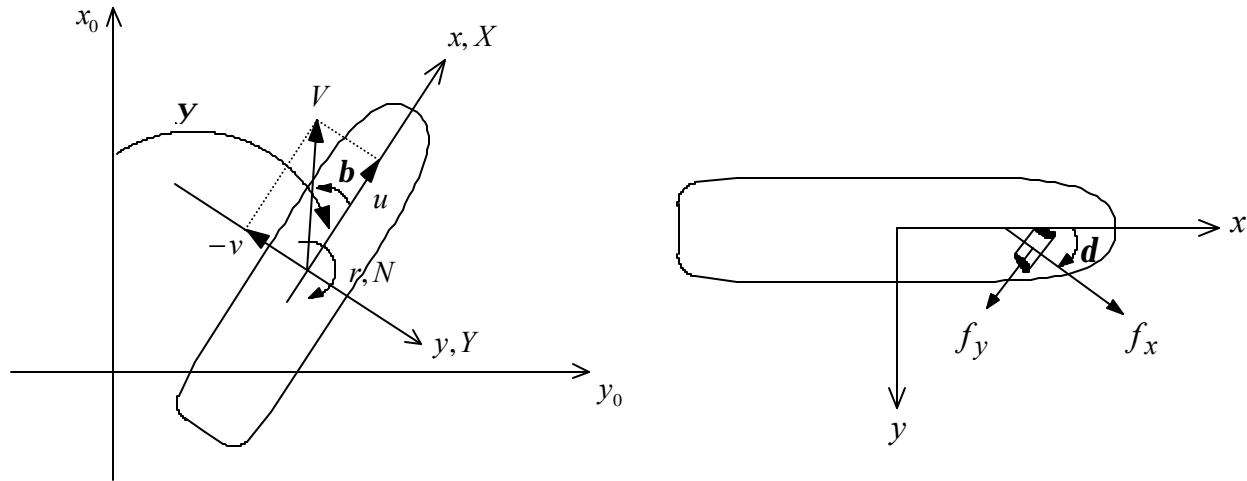


Figure 3 Coordinate system

4.3 Wind tunnel tests

The wind tunnel tests were performed on the above-water portions of the 1:200 scale model at the design draft with full setback on the drill floor. Wind speed in model scale was prudently chosen so that Reynolds No. effect was found negligible. The results of the tests were shown in Figure 4 where the force/moment coefficients are made non-dimensional as follows;

$$\begin{aligned} \text{Surge force} &: X'_W = X_W / 0.5\tilde{n}_a V_W^2 A_X \\ \text{Sway force} &: Y'_W = Y_W / 0.5\tilde{n}_a V_W^2 A_Y \\ \text{Yaw moment} &: N'_W = N_W / 0.5\tilde{n}_a V_W^2 A_Y L_{PP} \\ \text{where } \tilde{n}_a &: \text{air density} \\ V_W &: \text{wind speed} \\ A_X &: \text{front area of the vessel above water} \\ A_Y &: \text{side area of the vessel above water} \\ L_{PP} &: \text{length between perpendiculars} \end{aligned}$$

Vertical wind profile was set constant in the tests, wind forces in vertically-profiled shear flows can be, however, modified by calculations with use of height coefficient “Ch”, e.g. IMO MODU. Calculations of the wind forces are, therefore, available in various shear flows of various operating sites. As far as calculations of the derrick area are concerned, 60% of total derrick area is generally adopted in spite of area of setback pipes. Actual projected area of truss and setback pipes on the drill floor is, however,

adopted in the area calculations of A_x and A_y above so as to enable us to simulate the wind forces correctly against any quantity of the setback pipes. Of course, the truss area on both sides is taken into account according to the IMO MODU.

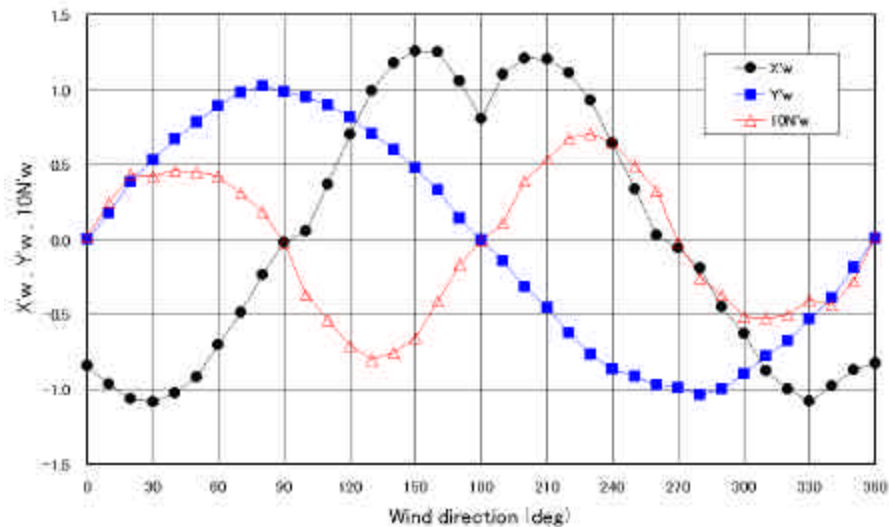


Figure 4 Wind force/moment coefficients

4.4 Wave drift force tests

The wave drift force tests were performed on the scale model of 1:65 at the design draft in long-crested irregular waves, for which Pierson-Moskowitz spectrum was applied. The other measurements than the wave drift forces were also carried out such as measurements of the vessel motion of six (6) degrees of freedoms, vertical accelerations, relative motion to wave surface, vertical force acting on the flange, which is installed on the side walls inside the moonpool in order to prevent the wave raise generated inside the moonpool during navigation. The coefficients of the wave drift force/moment are shown in Figure 5 and made non-dimensional as follows;

$$\begin{aligned}
 \text{Surge force} & : X'_D = X_D / 0.5\tilde{n}g\alpha_{1/3}^2 L_{PP} \\
 \text{Sway force} & : Y'_D = Y_D / 0.5\tilde{n}g\alpha_{1/3}^2 L_{PP} \\
 \text{Yaw moment} & : N'_D = N_D / 0.5\tilde{n}g\alpha_{1/3}^2 L_{PP}^2 \\
 \text{where } \tilde{n} & : \text{sea water density} \\
 g & : \text{acceleration of gravity} \\
 \alpha_{1/3} & : \text{significant wave amplitude}
 \end{aligned}$$

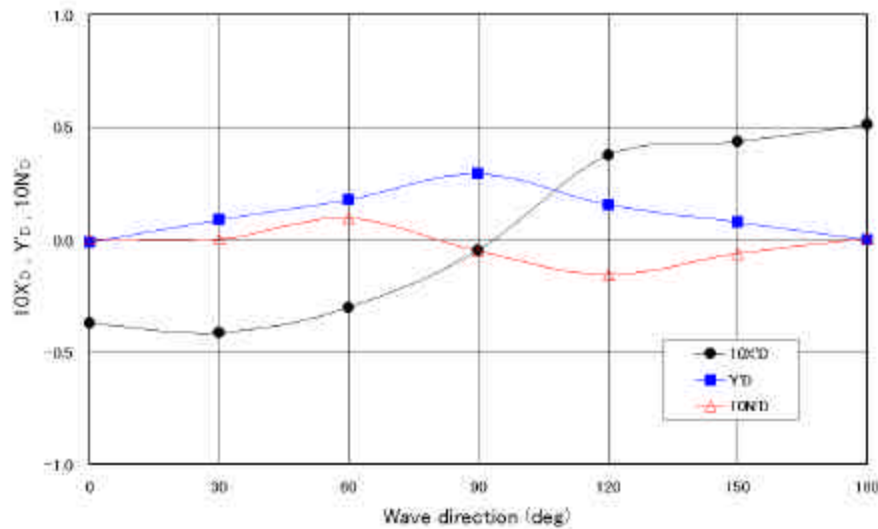


Figure 5 Wave drift force/moment coefficients ($T_{01}=8.2\text{sec}$: Drilling condition)

4.5 Current tests

The current tests were performed with and without the ducts of the azimuth thrusters at the design draft using the scale model same as the wave drift force tests. As the thrust used in the DP dynamic simulations include the drag of the ducts, the results without the ducts are applicable in the dynamic simulations. On the other hand, the results with the ducts are conservatively applied to the DP static simulations. The results of the tests are given in Figure 6 where the non-dimensional forces and moment are expressed as functions of the drift angle \hat{a} as follows;

$$\begin{aligned}
 \text{Surge force} & : X'_C(\hat{a}) = X_C / 0.5\tilde{n}V_C^2 L_{PP} d \\
 \text{Sway force} & : Y'_C(\hat{a}) = Y_C / 0.5\tilde{n}V_C^2 L_{PP} d \\
 \text{Yaw moment} & : N'_C(\hat{a}) = N_C / 0.5\tilde{n}V_C^2 L_{PP}^2 d \\
 \text{where } V_C & : \text{current speed} \\
 d & : \text{draft} \\
 \hat{a} & : \text{drift angle (current direction)}
 \end{aligned}$$

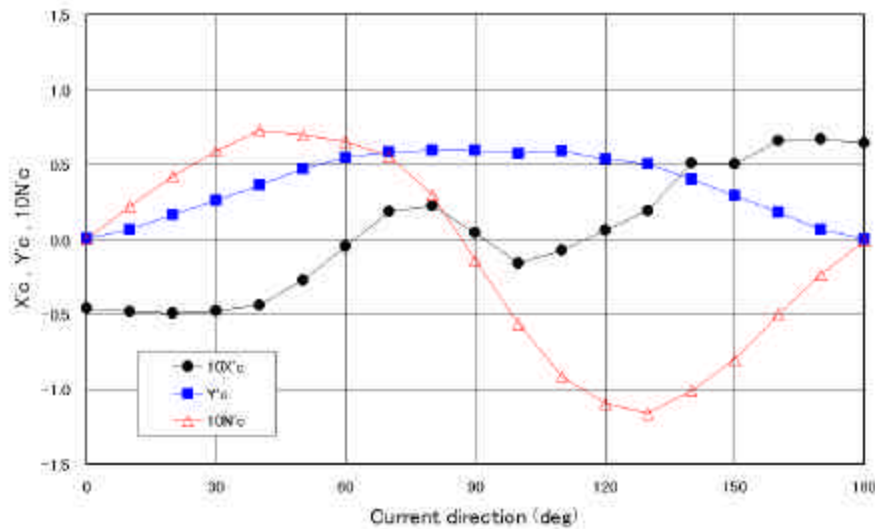


Figure 6 Current force/moment coefficients

4.6 Yaw-rotating tests and thruster interaction tests

The hydrodynamic forces acting on the hull due to vessel horizontal motion are assumed to be composed of three parts as follows;

$$\begin{aligned}
 \text{Surge force} & : X_H = X_{H1}(\hat{a}) + X_{H2}(r) + X_{H3}(u, v, r) \\
 \text{Sway force} & : Y_H = Y_{H1}(\hat{a}) + Y_{H2}(r) + Y_{H3}(u, v, r) \\
 \text{Yaw moment} & : N_H = N_{H1}(\hat{a}) + N_{H2}(r) + N_{H3}(u, v, r)
 \end{aligned}$$

The terms with subscript H1 represent the hull forces due to pure drifting motion only, namely those are the same as the current forces X_C , Y_C and N_C mentioned above. The terms with subscript H2 and H3 represent the hull forces respectively due to pure turning motion only and due to coupling effect between pure drifting and turning motion. The forces with subscript H2 and H3 were obtained from the yaw-rotating tests, in which the scale model was towed at a constant speed while rotating around the vertical axis through the midship with a constant yaw angular velocity⁷⁾. It was found from the yaw-rotating tests that the mathematical model for the hull forces is given by;

$$\begin{aligned}
 \text{Surge force} & : X_H = \{X'_C(\hat{a}) + X'_{vr}v'r' + X'_{rr}r'^2\} & \square 0.5\tilde{n}V^2 L_{PP}d \\
 \text{Sway force} & : Y_H = \{Y'_C(\hat{a}) + Y'_{ur}u'r' + Y'_{ur|r}u'r'|r'| + Y'_{v|r}v'|r'|\} & \square 0.5\tilde{n}V^2 L_{PP}d \\
 \text{Yaw moment} & : N_H = \{N'_C(\hat{a}) + N'_{r}r' + N'_{r|r}r'|r'| + N'_{v|r}v'|r'|\} \\
 & \quad + N'_{vvr}v'v'r' + N'_{uv|r}u'v'|r'|\} & \square 0.5\tilde{n}V^2 L_{PP}^2d
 \end{aligned}$$

$$\begin{aligned}
 \text{where } u & : \text{surge velocity relative to water}(u'=u/V) \\
 v & : \text{sway velocity relative to water}(v'=v/V) \\
 V & : \text{vessel speed}(=(u^2+v^2)^{1/2}) \\
 r & : \text{yaw angular velocity}(r'=rL_{PP}/V)
 \end{aligned}$$

The forces and moment due to operation of the azimuth thrusters can be expressed by;

$$\text{Surge force} : X_T = \sum_{i=1}^6 \{ \dot{a}_{xi} \square fx \square \cos \ddot{a}_i - \dot{a}_{yi} \square fy \square \sin \ddot{a}_i \}$$

$$\text{Sway force} : Y_T = \sum_{i=1}^6 \{ \dot{a}_{xi} \square fx \square \sin \ddot{a}_i + \dot{a}_{yi} \square fy \square \cos \ddot{a}_i \}$$

$$\text{Yaw moment: } N_T = \sum_{i=1}^6 [-\{ \dot{a}_{xi} \square fx \square \cos \ddot{a}_i - \dot{a}_{yi} \square fy \square \sin \ddot{a}_i \} y_i + \{ \dot{a}_{xi} \square fx \square \sin \ddot{a}_i + \dot{a}_{yi} \square fy \square \cos \ddot{a}_i \} x_i]$$

where fx : longitudinal force in the direction of the propeller shaft including the thruster-current interference effects

fy : transverse force in the direction perpendicular to the propeller shaft including the thruster-current interference effects

\ddot{a}_i : deflection angle of the i -th azimuth thruster

$\dot{a}_{xi}, \dot{a}_{yi}$: thruster-hull interference coefficient for the i -th azimuth thruster

The thruster-current interaction tests were performed in open water for the individual azimuth thruster without the hull. Figure 7 shows the thruster-current interference effects, e.g. the non-dimensional longitudinal force $f'x$ as function of the advance angle for various deflection angle \ddot{a} . The thruster-hull interference effects were obtained from the thruster-hull interaction tests, which were performed on the ship model equipped with six(6) azimuth thrusters. Figure 8 shows the thruster-hull interference coefficients, e.g. \dot{a}_x , as function of the deflection angle for the thruster located at fore-starboard. In addition, the thruster-thruster interaction tests were also executed between two (2) azimuth thrusters on both sides for respectively fore and aft combinations.

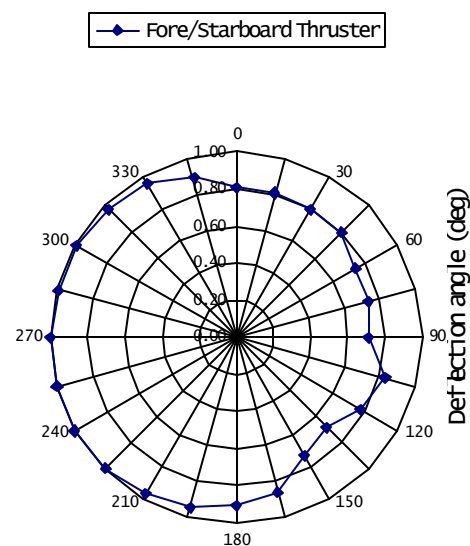
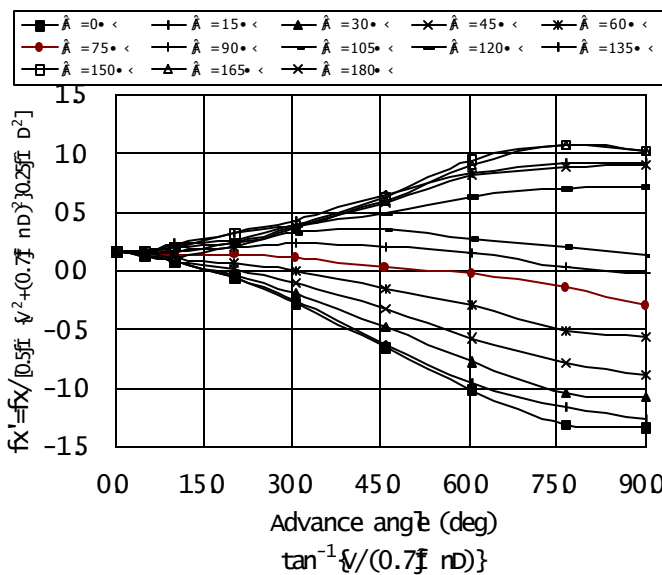


Figure 7 Thruster force coefficients $f'x$

Figure 8 Thruster-hull interference coefficients \dot{a}_x

5 DP control tests

5.1 Overview

The mathematical model for dynamic simulations was constructed with such data obtained by the above-mentioned model tests. In order to confirm validity of the mathematical model and the DP control algorithm including the thrust allocation for the six (6) azimuth thrusters, DP control tests were performed at the current water tank of the Akishima Laboratories (Mitsui Zosen) Inc., dimensions of which are length 55m x breadth 8m x water depth 2.5m. The model used in the tests is a 1:55 scale model with six (6) azimuth thruster models, shown in [Figure 9](#).



Figure 9 Model for DP control test

The test conditions are given in [Table 3](#). In the positioning tests, the model was controlled so as to maintain heading as well as position in wind, wave and current and also in the turning tests the model was controlled to turn by 360 degrees with a constant yaw angular velocity while maintaining vessel position.

Table 3 Environmental conditions for the DP control test

Kind of test	Positioning						Turning
	1	2	3	4	5	6	
Case No.							7
Condition	Drilling	Drilling	Standby 1	Standby 2	Drilling	Standby 2	
Wind speed V _{w_1min} (m/s)	23	23	30	23	23	23	15
Wave height H _{1/3} (m)	4.5	4.5	5.5	5.5	4.5	5.5	3.5
Wave period T ₀₁ (sec)	8.2	8.2	9.0	9.0	8.2	9.0	7.2
Current speed (kts)	1.5	1.5	1.5	2.5	1.5	2.5	1.5
Wind direction (deg)	30	30	30	30	210	210	30
Wave direction (deg)	0	0	0	0	180	180	0
Current direction (deg)	0	0	0	0	180	180	0
Thruster out of order	Tunnel	Tunnel	Tunnel	Tunnel	Tunnel	Tunnel	Tunnel
		Azimuth Fore Center			Azimuth Aft Starboard		

(Note) Wind / wave / current direction of zero(0) degree indicates the bow into the environment.

Every value is represented in full scale.

The DP control system for the model tests includes PID controller, Kalman filter algorithm, feedforward controller for compensating wind forces and azimuth thruster allocation logic, which are the same as those to be installed for the full-scale OD21 drillship. In particular, the azimuth thruster allocation logic determines optimum distribution of thrust and deflection angle for six (6) azimuth thrusters. The thrust and deflection angle for each azimuth thruster, i.e. twelve (12) quantities in all, are determined by Lagrange's method of multipliers so as to minimize the following cost function. Whenever a control order was issued by the DP control system, this equation was solved by every time step, i.e. approx. 0.07second in model scale corresponding to 0.5second in full scale.

$$J(X_{Ti}, Y_{Ti}) = w_i (X_{Ti}^2 + Y_{Ti}^2) \quad i = 1 \text{ to } 6$$

where X_{Ti} : Surge force of the i -th azimuth thruster
 Y_{Ti} : Sway force of the i -th azimuth thruster
 w_i : weighting parameter for the i -th azimuth thruster

In the tests, heading and position of the model were measured by a video tracking system. Long-crested irregular waves and fluctuating wind were generated respectively by a plunger-type wave maker and four(4) wind fans. The waves and wind were composed of the Pierson-Moskowitz and Harris spectrum respectively. **Figure 10** shows a general view of the DP control tests and **Figure 11** gives a schematic diagram of the measuring system.



Figure 10 General view of the DP control test

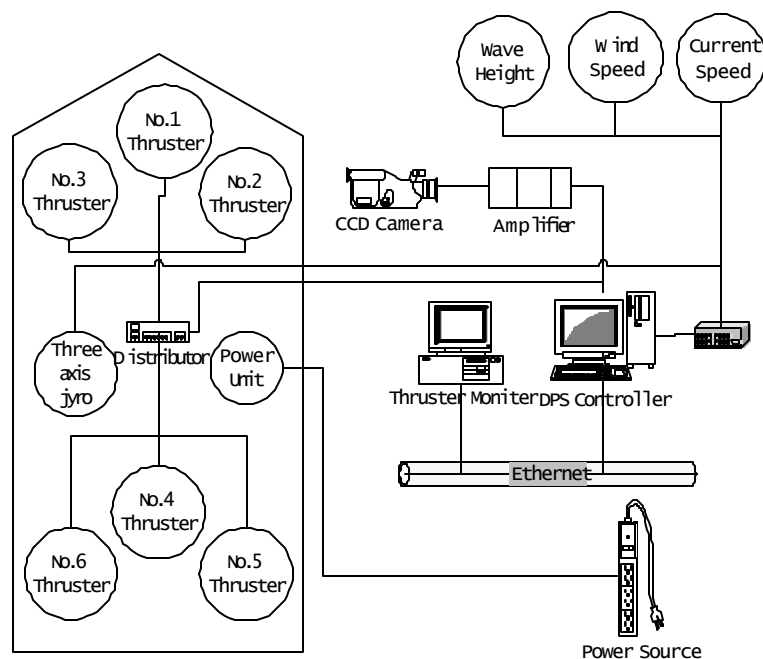


Figure 11 Schematic diagram of measuring system

5.2 Positioning tests

The vessel trajectories measured in the tests of CASE No.2 and No.4 are given in [Figures 12](#) and [13](#) respectively as typical examples of the tests. It can be seen from both figures that the model maintained the target position within deviation of 15m drawn by a circle. The allowable excursion is 15m for the drilling condition, e.g. CASE No.2, and 30m for the standby conditions, e.g. CASE No.4, as indicated in [Table 2](#). [Table 4](#) gives the summary of 2σ (σ: standard deviation) for heading and position measured in the positioning tests.

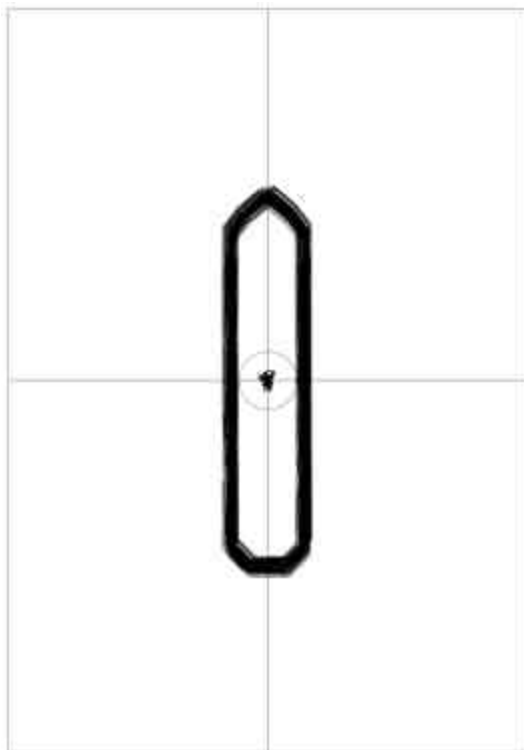


Figure 12 Vessel trajectory measured in positioning test of CASE No.2

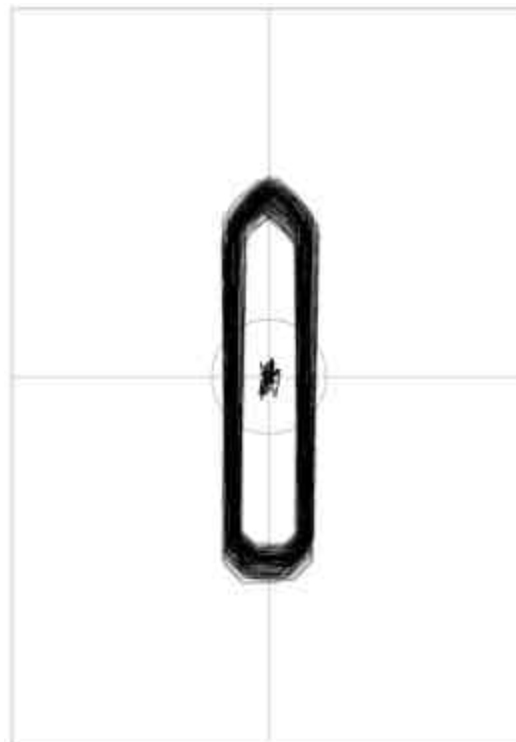


Figure 13 Vessel trajectory measured in positioning test of CASE No.4

Table 4 Summary of 2σ in positioning tests

Case No.	1	2	3	4	5	6
Condition	Drilling	Drilling	Standby 1	Standby 2	Drilling	Standby 2
2σ for heading (deg)	0.9	0.9	1.4	1.5	0.9	1.5
2σ for position (m)	5.6	5.7	7.8	10.8	7.6	11.9

The test results show that the vessel was able to maintain her heading and position with sufficient accuracy, namely within the allowable excursion, even in the standby conditions. These results of 2σ were a little higher than previously estimated mainly due to fluctuations of current speed during the tests. As fluctuating period was close to the natural period of “Hull+DPS”, this effect was not negligible. From the dynamic simulations with and without considerations of the fluctuating current, it is found that the fluctuating current gives vessel’s excursion a higher value by approx. 2 to 3m in 2σ than without the fluctuation. I.e. it is assumed that a little lower 2σ than the model tests might be achieved in full-scale DP control without current fluctuations.

Although [Table 4](#) shows $\dot{\phi}$ for the steady control after terminating transient motion of the vessel just after so called “cold start” of the DPS, sudden failure of one(1) azimuth thruster was demonstrated for both cases of “one(1) azimuth thruster out of order”, i.e. CASE No.2 and 5. From these tests, it was proved that the DP controller, especially the azimuth thruster allocation logic, was capable of countering such sudden failures quickly and correctly and that the failure did not influence accuracy of the heading and positioning at all. It is concluded from the test results above that the DP control system works satisfactory and can be successfully applied to the full-scale vessel.

5.3 Turning tests

In order to confirm that the vessel is able to turn by 360 degrees while maintaining her position in environment, the turning tests were performed. Preliminary tests were done to determine the yaw angular velocities for maintaining the vessel position within a circle with radius of 15m. As a result the yaw angular velocity of 3 deg/min was applied for the tests. [Figure 14](#) shows the vessel trajectory measured during the turning from 360 to 270 deg. The results showed that the vessel was able to turn by 360 degrees successfully while maintaining her position in a relatively high environment.

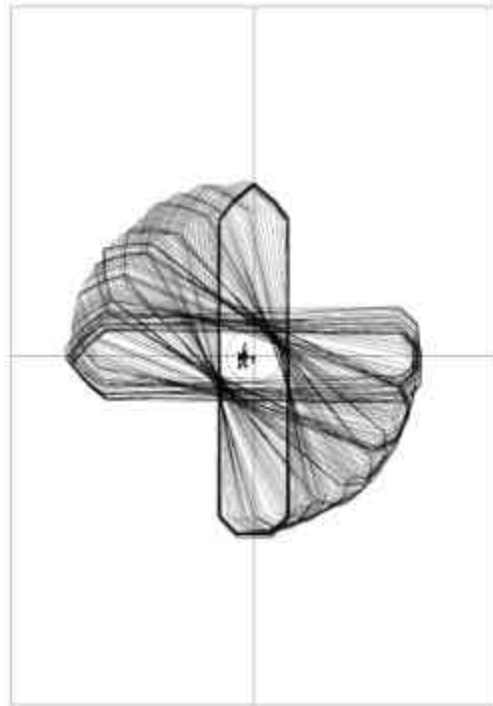


Figure 14 Vessel trajectory measured in turning tests

5.4 Comparisons between tests and simulations

In order to verify applicability of the simulations based on the mathematical model mentioned above, a series of simulation corresponding to the test program was performed. The simulations take account of the wave/wind spectrums applied to the model tests so that the vessel motion due to the long-crested irregular waves and fluctuating wind precisely appear in the simulations. The simulated vessel trajectory for CASE No.2 is given in [Figure 15](#). In [Figures 16 and 17](#), the average RPM and deflection angles of the azimuth thrusters simulated for CASE No.2 and CASE No.4 respectively are compared with those measured in the tests. Good correlation between the simulation and test results can be seen for both vessel trajectories and azimuth thruster operations. The model tests prove that accuracy of the simulation has been verified and also that the simulation is a practically useful tool for evaluating the DPS of the vessel.

Figure 15 Simulated vessel trajectory for CASE No.2

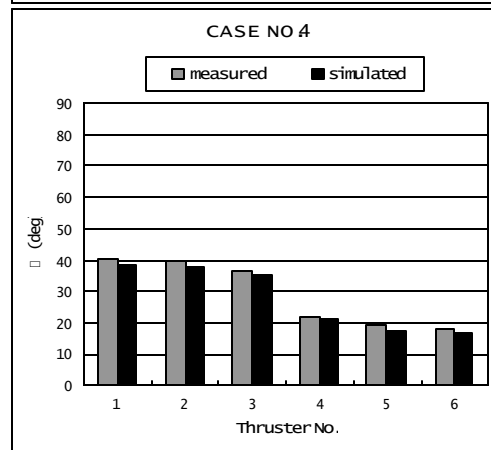
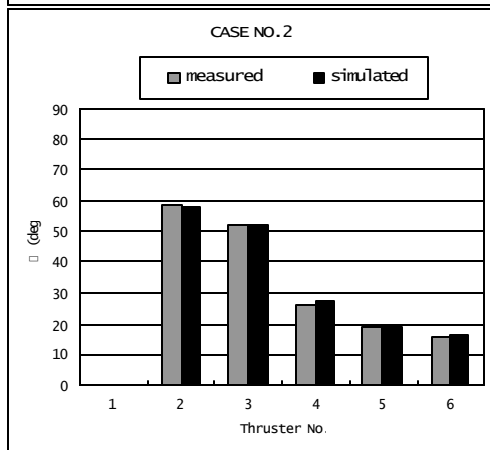
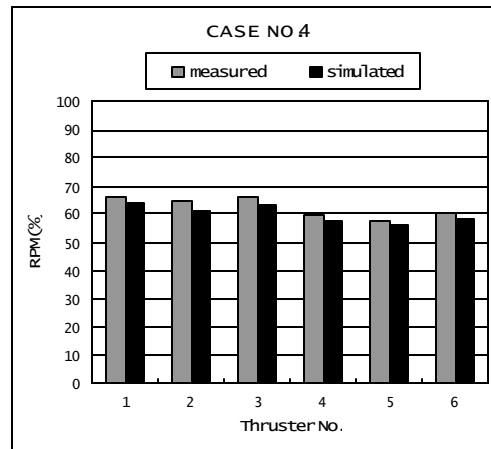
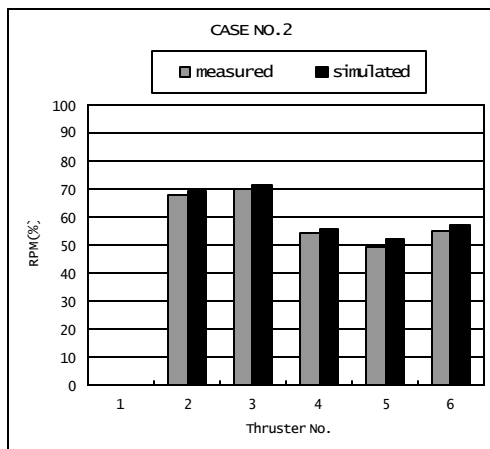
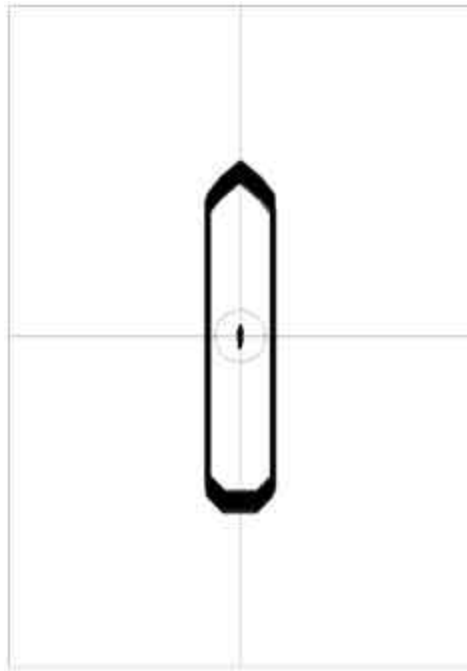


Figure 16 Comparisons between simulation and test results for CASE No.2

Figure 17 Comparisons between simulation and test results for CASE No.4

6 Conclusion

During the basic design stage of the DPS, the various model tests were successfully performed with the actual DP control system without “a black box” on the DP control. As a matter of fact, the DPS of the OD21 drillship has been developed based on an intellect and experience of the parties concerned with use of the model test results. The DPS is one of the key technologies of the vessel and then integration of such technologies being developed for the project is expected to contribute to developments of the physical geography of the Earth and moreover to give a solution against an essential question “What is the Earth?”. The OD21 drillship shall, we hope, sail into the 21st century with lots of dreams and expectations all over the world.

References

- 1) Takagawa, S., Sakai, D., Ozawa, H. and Yamamoto, H. : Overview of the OD 21 Project, Bulletin of The Society of Naval Architects of Japan, March 1999 (in Japanese)
- 2) Imakita, A., Tanaka, S., Amitani, Y. and Takagawa, S. : Intelligent riser angle control DPS, OMAE, New Orleans, 1999
- 3) Imakita, A., Tanaka, S., Amitani, Y. and Takagawa, S. : Intelligent riser angle control DPS, DP Conference, Houston, October 2000
- 4) Takaishi, Y., Matsumoto, T. and Ohmatsu, S. : Winds and waves of the North Pacific Ocean, Papers of Ship Research Institute, 1980
- 5) Garcia, J.C.L., and Michel, R.P. : Naval architectural design of a 5th generation drillship, 9th Deep Ocean Technology, The Hague, 1997
- 6) Schoonmade, W., Janse, W., Lusthof, J. and Rietveldt, B. : A new generation DP drillships, Gusto 10000 and Gusto P-10000, Ocean Technology Conference, 1998
- 7) Takashina, J. : Ship maneuvering motion due to tugboats and its mathematical model, Journal of the Society of Naval Architects of Japan Vol.160, 1986